Stem Cell Reports
Report
ISSCR
OPEN ACCESS

# Endoderm Generates Endothelial Cells during Liver Development

Orit Goldman,[1,4] Songyan Han,[1,4] Wissam Hamou,[1] Vanina Jodon de Villeroche,[2] Georges Uzan,[2] Heiko Lickert,[3] and Valerie Gouon-Evans[1,*]
[1]Department of Developmental and Regenerative Biology, Black Family Stem Cell Institute, Icahn School of Medicine, Mount Sinai, New York, NY 10029, USA
[2]INSERM U972, Hospital Paul Brousse, 12 Avenue Paul Vaillant Couturier, 94807 Villejuif, France
[3]Institute of Diabetes and Regeneration Research, Helmholtz Zentrum München, 85764 Neuherberg, Germany
[4]Co-first author
*Correspondence: valerie.gouon-evans@mssm.edu
http://dx.doi.org/10.1016/j.stemcr.2014.08.009


## SUMMARY

Organogenesis requires expansion of the embryonic vascular plexus that migrates into developing organs through a process called angiogenesis. Mesodermal progenitors are thought to derive endothelial cells (ECs) that contribute to both embryonic vasculogenesis and the subsequent organ angiogenesis. Here, we demonstrate that during development of the liver, which is an endoderm derivative, a subset of ECs is generated from FOXA2+ endoderm-derived fetal hepatoblast progenitor cells expressing KDR (VEGFR2/FLK-1). Using human and mouse embryonic stem cell models, we demonstrate that KDR+FOXA2+ endoderm cells developing in hepatic differentiation cultures generate functional ECs. This introduces the concept that ECs originate not exclusively from mesoderm but also from endoderm, supported in *Foxa2* lineage-tracing mouse embryos by the identification of FOXA2+ cell-derived CD31+ ECs that integrate the vascular network of developing fetal livers.

## INTRODUCTION

In early development, endothelial cells (ECs) emerge from mesodermal progenitors and initiate vasculogenesis to form the extraembryonic yolk sac vasculature and the embryonic primary vascular plexus. Subsequently, these vascular systems are rapidly expanded and remodeled. This process is termed "angiogenesis" and involves endothelial sprouting, vessel branching, and intussusception from existing blood vessels (Patan, 2004). Hepatic blood vessels consist of the hepatic artery and three types of venous vessels (the portal veins, hepatic veins, and sinusoids) that differentiate as the liver bud expands around embryonic day 10.5 (E10.5) in the mouse embryo. Based on the position of the hepatic vessels and differential expression of connexins and the NOTCH ligand Jagged1, the origin of the hepatic endothelium was proposed to be the adjacent vasculature, including omphalomesenteric veins for the portal veins (Shiojiri et al., 2006), the cardinal vein and the sinus venosus for the hepatic veins (Shiojiri et al., 2006), and the omphalomesenteric and cardinal veins for the sinusoids (Sugiyama et al., 2010). Although interpretations from studies seeking to define the precise origins of the hepatic vasculature differ, the dogma is that the hepatic endothelium is of mesodermal origin.

We provide evidence that fetal hepatic ECs also originate from a hepatic endoderm progenitor that expresses the vascular endothelial growth factor (VEGF) receptor KDR (VEGFR2/fetal liver kinase 1). Our previous work revealed the existence of KDR-expressing hepatic progenitors (KDR+ progenitor) in human embryonic stem cell (hESC) cultures differentiated toward the hepatic lineage (Goldman et al., 2013). Isolated hESC-derived endoderm cells give rise to both the KDR+ hepatic progenitors and the committed KDR− hepatic cells. A subset of ECs coexpressing KDR and the endothelial marker CD31 (platelet endothelial cell adhesion molecule) consistently developed in hepatic differentiated cultures. KDR+ progenitors are conserved in the developing liver of the mouse because they are present in E8.0 mouse anterior foregut endoderm, confirmed by cell morphology and expression of the endoderm marker FOXA2. Foregut endoderm cells coexpressing KDR and FOXA2 generated in fetal livers a large subset of progenitors for hepatocytes and cholangiocytes, the fetal hepatoblasts, which in turn derived hepatocytes and cholangiocytes in adult livers. Here, we demonstrate that KDR+ hepatic progenitors are also an unexpected endoderm-derived progenitor for ECs that develop concomitantly with hepatic cells in human and mouse ESC hepatic differentiation cultures. Two lineage-tracing studies in mice tracking the fate of FOXA2-expressing cells provide in vivo evidence for the EC fate of FOXA2+ cells in the developing fetal liver, supporting the concept that ECs in the fetal liver can also originate from an endoderm derivative.

## RESULTS

### Identification of Human ECs Generated from hESC-Derived KDR+ Endoderm Cells and Human Fetal Livers

Following induction with a high dose of Activin A in embryoid body (EB) cultures, an enriched cell population

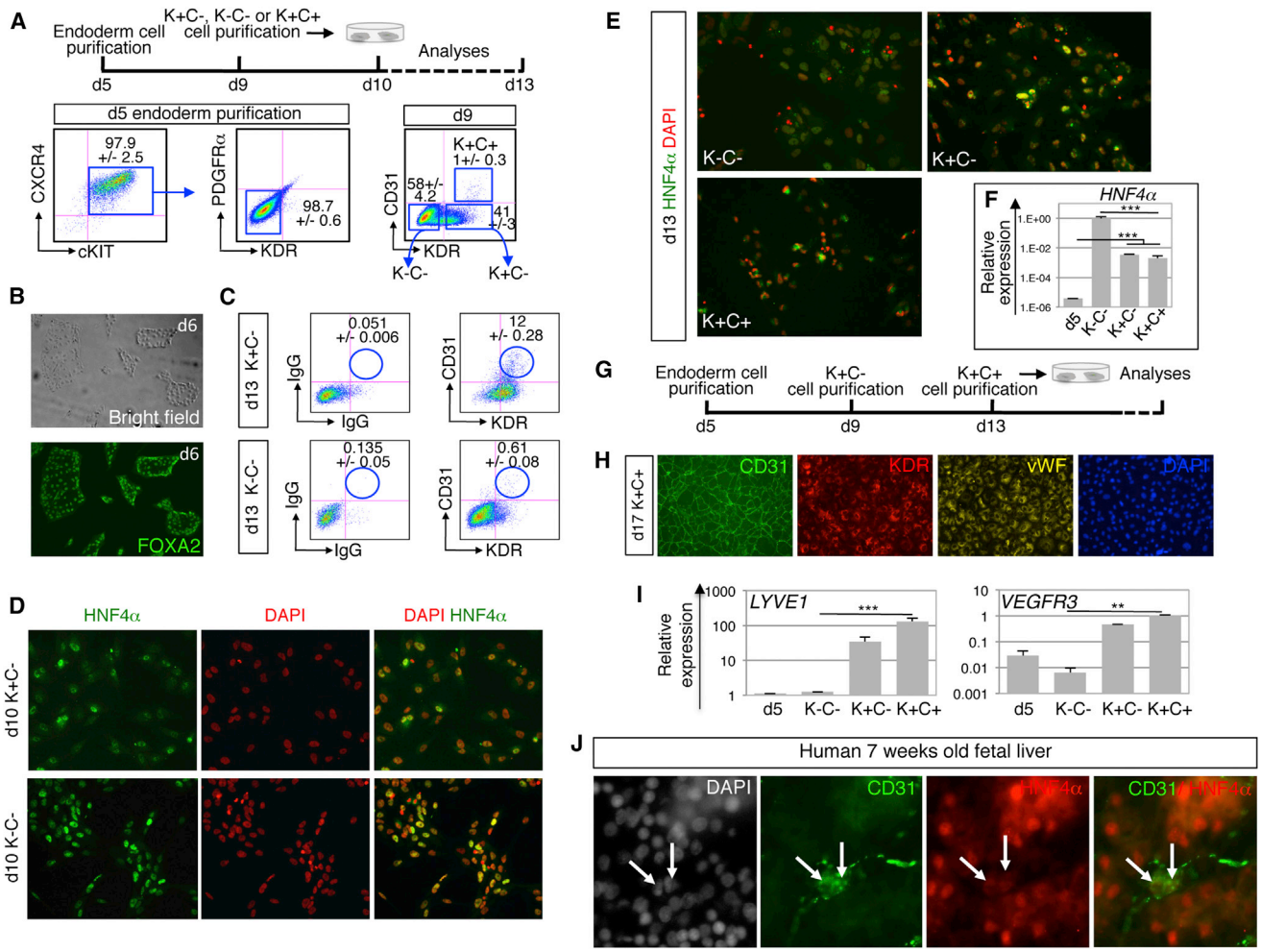


**Figure 1. Generation of ECs from hESC-Derived KDR+ Endoderm Cells**

(A) Flow analysis from day 5 EBs and day 9 hepatic cultures generated from the plated day 5 CXCR4+cKIT+KDR-PDGFRα− (endoderm) cells. All numbers reflect the mean ± SD for the number ("n") of independent experiments (n = 5).

(B) Bright-field and FOXA2 IF image of day 5 endoderm cells cultured for 1 day (×200).

(C) Flow analysis at day 13 of K+C− and K−C− cells purified at day 9 (n = 3).

(D) IF of day 9 K+C− and K−C− populations 1 day after plating (×200).

(E) IF of day 9 K−C−, K+C−, and K+C+ populations 4 days after plating (×200).

(F) qPCR analyses for *HNF4α* levels in day 5 endoderm population, and K−C−, K+C−, and K+C+ populations cultured for 4 days (n = 4).

(G) Purification and expansion of K+C+ cells from day 9 K+C− cells.

(H) IF of K+C+ cells cultured to day 17 (×200).

(I) qPCR analyses in day 5 endoderm population, and K−C−, K+C−, and K+C+ populations cultured for 4 days (n = 4).

(J) Co-IF for CD31 and HNF4α on 7-week-old human fetal liver sections (×200). Arrows indicate cells coexpressing CD31 and HNF4α.

positive for the endoderm markers CXCR4 and cKIT and negative for KDR and the mesendodermal marker platelet-derived growth factor receptor α (PDGFRα) was generated with high efficiency (Figure 1A). These cells were isolated using fluorescence-activated cell sorting (FACS) at day 5 of differentiation with purity above 95% (Figure S1A available online). PDGFRα is expressed on nearly all cells at day 4 of differentiation (Goldman et al., 2013) but is completely downregulated by day 5 of differentiation (Figure 1A), so that the day 5 CXCR4+cKIT+ population is staged beyond mesendoderm development. To verify purity of endoderm cells, immunofluorescence (IF) staining for the endoderm marker FOXA2 was performed after 1 day of culture. Endoderm cells formed clusters in which each cell expresses FOXA2 (Figure 1B). In hepatic media, the endoderm cells gave rise sequentially to hepatic progenitors (KDR+CD31−, hereafter termed "K+C−"), the hepatic cells (KDR-CD31−, hereafter termed "K−C−"),

and finally a small subset of endothelial-like cells (KDR+CD31+, hereafter termed "K+C+") (Figure 1A) (Goldman et al., 2013). The true identity of K+C− hepatic progenitors was shown by their ability following hepatic maturation to support hepatitis C virus infection, a unique feature for hepatocytes (Goldman et al., 2013).

To determine the origin of the K+C+ ECs, K+C− progenitors and K−C− hepatic cells were isolated at day 9 of differentiation (Figure 1A) with purity always higher than 97% (Figure S1B), cultured for 4 additional days in hepatic media, and then evaluated for the generation of ECs based on CD31 and KDR expression (Figure 1C). Only the K+C− cells were able to generate K+C+ ECs (Figure 1C).

To verify that ECs originate from endoderm-derived K+C− cells, we examined expression of hepatocyte nuclear factor 4 α (HNF4α), the main transcription factor regulating endoderm hepatic specification (Parviz et al., 2003), and of the epithelial markers CK18 and CK19, which are expressed on human hepatoblasts (Roskams and Desmet, 2008). One day following the purification of day 9 K+C− cells, virtually all K+C− cells expressed HNF4α (Figure 1D) and both CK18 and CK19 (Figure S1C). Purified K−C− hepatic cells served as positive control for the three markers (Figures 1D and S1C). Comparison of HNF4α protein (Figure 1E) and transcript (Figure 1F) levels among purified K−C−, K+C−, and K+C+ populations cultured for 4 days showed the highest and most homogeneous expression of HNF4α protein in hepatic K−C− cells, whereas distribution of HNF4α protein becomes heterogeneous in K+C− progenitor cells and even more patchy in K+C+ ECs. Levels of *HNF4α* transcript paralleled protein levels and indicated highest levels in K−C− hepatic cells and lower similar levels in K+C− progenitors and K+C+ ECs. Although lower than seen in K−C− cells, *HNF4α* levels in K+C− and K+C+ populations were significantly higher than in day 5 endoderm cells. The presence of residual HNF4α in K+C+ ECs further supports their endodermal origin.

The endothelial identity of K+C+ cells was supported by expression of an additional endothelial marker, TIE2, evaluated as they emerged from purified K+C− cell populations (Figure S1D). As the K+C− cells differentiate into ECs, most of the K+C+ ECs expressed TIE2. Moreover, all K+C+ cells purified from cultured K+C− cells (Figure 1G) coexpressed the cytoplasmic marker for EC maturation, von Willebrand factor (vWF), and the cell surface markers CD31 and KDR (Figures 1H and S1E). The endothelial phenotype of K+C+ cells was stable because K+C+ cells continued to express CD31, KDR, and the endothelial marker CD144 (vascular endothelial [VE]-cadherin) following three passages (Figure S1F). Furthermore, high levels of transcripts for the sinusoidal endothelial markers *LYVE-1* and *VEGFR3* (Ding et al., 2010; Nonaka et al., 2007) (Figure 1I) were found in K+C+ cells as compared to K−C− and K+C− populations. Homogeneous expression of LYVE1 protein in K+C+ cells was confirmed, whereas the percentage of K+C+ cells expressing VEGFR3 protein was low, indicating discrepancy between transcript and protein levels for VEGFR3 (Figure S1F). These molecular assays suggest a more specialized sinusoidal phenotype of the endoderm-derived K+C+ ECs.

To identify endoderm-derived ECs in early human development, we searched human fetal liver specimens for ECs that coexpressed CD31 and HNF4α, as characterized in hESC cultures. We identified a few CD31+HNF4α+ ECs in 7- and 7.5-week-old fetal livers, which approximates the developmental stage of hESC hepatic cultures (Figures 1J and S1G–S1I). These double-positive cells suggest the presence of ECs derived from endoderm in developing human fetal livers.

## K+C+ ECs Derived from hESC-Derived KDR+ Endoderm Cells Are Functional In Vitro and In Vivo

We performed four well-established in vitro EC functional assays (Goldman et al., 2009) to evaluate and compare functionality of the purified K+C+ ECs generated from hESC-derived endoderm cells to primary human umbilical vascular ECs (HUVECs). K+C+ cells behaved similarly to HUVECs in all assays. Their migratory rates were similar in a wound-healing assay (Figure 2A). K+C+ cells incorporated acetylated low-density lipoprotein (ac-LDL) (Figure 2B) and formed tubes when placed into thick Matrigel (Figure 2C). Finally, the vast majority of K+C+ cells induced vascular cell adhesion molecule (VCAM), intercellular adhesion molecule (ICAM), and E-selectin membrane expression following tumor necrosis factor α (TNF-α) stimulation (Figures 2D and S2A).

To demonstrate in vivo functionality of K+C+ ECs, K+C− progenitors were transplanted into an injured muscle of nonobese diabetic/severe combined immunodeficiency mice that underwent femoral artery ligation inducing de novo angiogenesis. An antibody against human CD31 (hCD31) was used to detect K+C+ ECs generated from the transplanted K+C− progenitors. Functionality of the K+C+ ECs was assessed by the visualization of hCD31+ cells integrated in the repaired host vessels by the presence of GFP-labeled dextran present in all diffused functional vessels. One week following K+C− cell transplantation, many hCD31+ cells were identified within diffused vessels that were stained with dextran-GFP, indicating that the K+C− transplanted cells generated functional K+C+ ECs in vivo (Figures 2E–2G, arrows). The human specificity of the hCD31 antibody was confirmed by the absence of staining of GFP-labeled dextran mouse ECs in control non-transplanted injured muscle (Figure 2H). These data identified a subset of ECs that develop from the hESC-derived KDR-expressing hepatic progenitor.

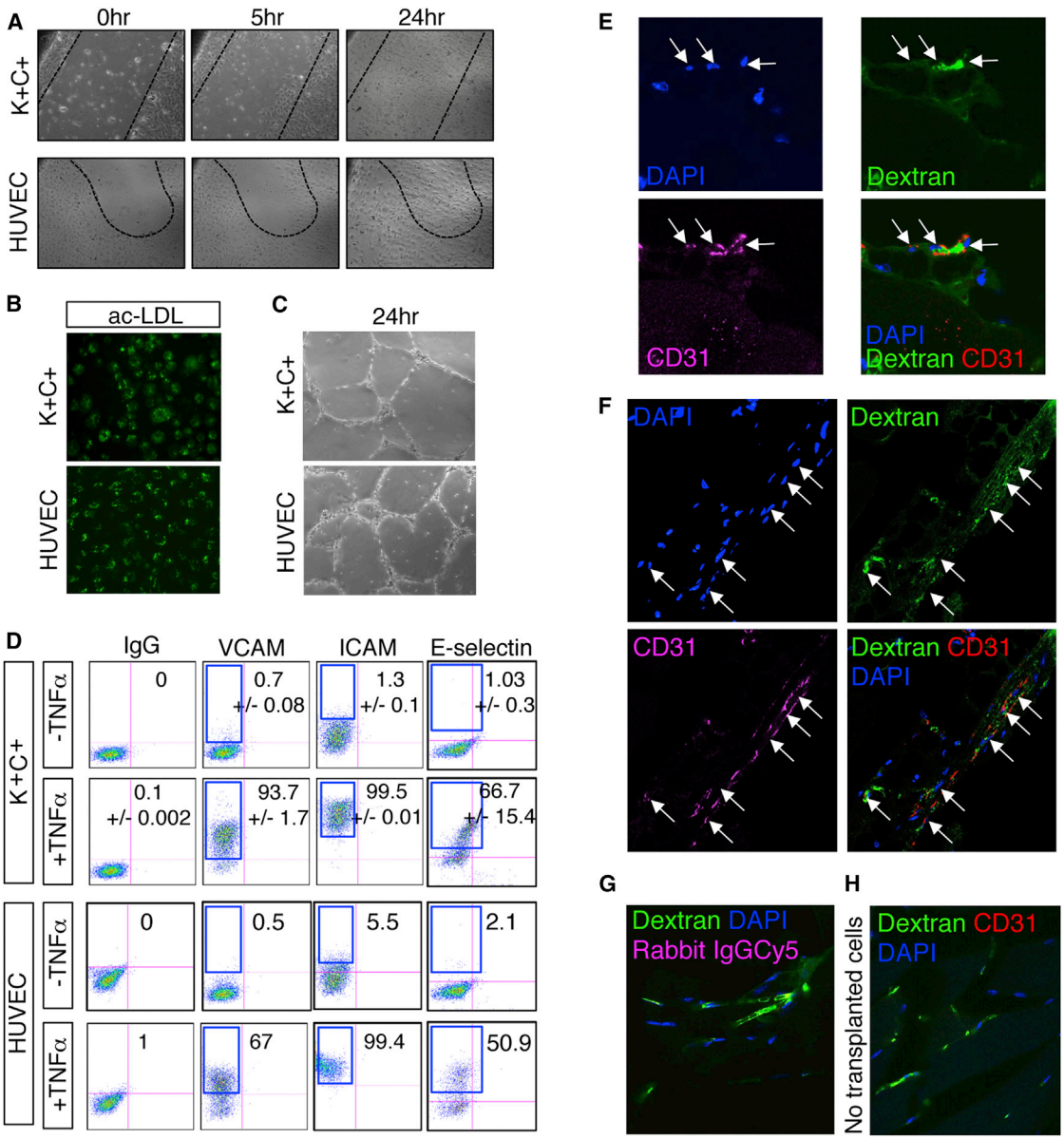


**Figure 2. In Vitro and In Vivo Functions of K+C+ ECs Generated from hESC-Derived K+C− Progenitors**

(A–D) Comparison of in vitro functions of K+C+ cells with HUVECs in a wound assay (×200) (A), incorporation of ac-LDL (×200) (B), tube formation assay in Matrigel (×200) (C), and VCAM, ICAM, and E-Selectin expression analyzed by flow following TNF-α activation (n = 3 independent experiments) (D). IgG, immunoglobulin G.

(E–H) In vivo function of K+C+ cells generated from K+C− cells transplanted into a femoral artery ligation injury mouse model. Dextran-GFP was injected 5 min prior to sacrifice to visualize the functional diffused GFP+ vessels. IF for hCD31 1 week after cell transplantation is shown. Arrows indicate the transplanted hCD31+ ECs that integrated the GFP host mouse vessels. Close-up pictures are from ×200.

## Identification of Mouse ECs Generated from Mouse ESC-Derived KDR+ Endoderm Cells

To determine whether the development of ECs from an endoderm progenitor was conserved in the mouse, we first identified in vitro the emerging FOXA2+ endoderm cells expressing KDR upon hepatic specification of an anterior primitive streak-like mouse ESC-derived cell population. The endoderm program was induced with a high dose of Activin A using a dual-reporter mouse ESC line in which GFP and human CD4 cDNAs were targeted to the *Brachyury* (*T*) and *Foxa2* loci, respectively (*T*-GFP, *Foxa2*-CD4) (Gouon-Evans et al., 2006). At day 5 of differentiation, most of the

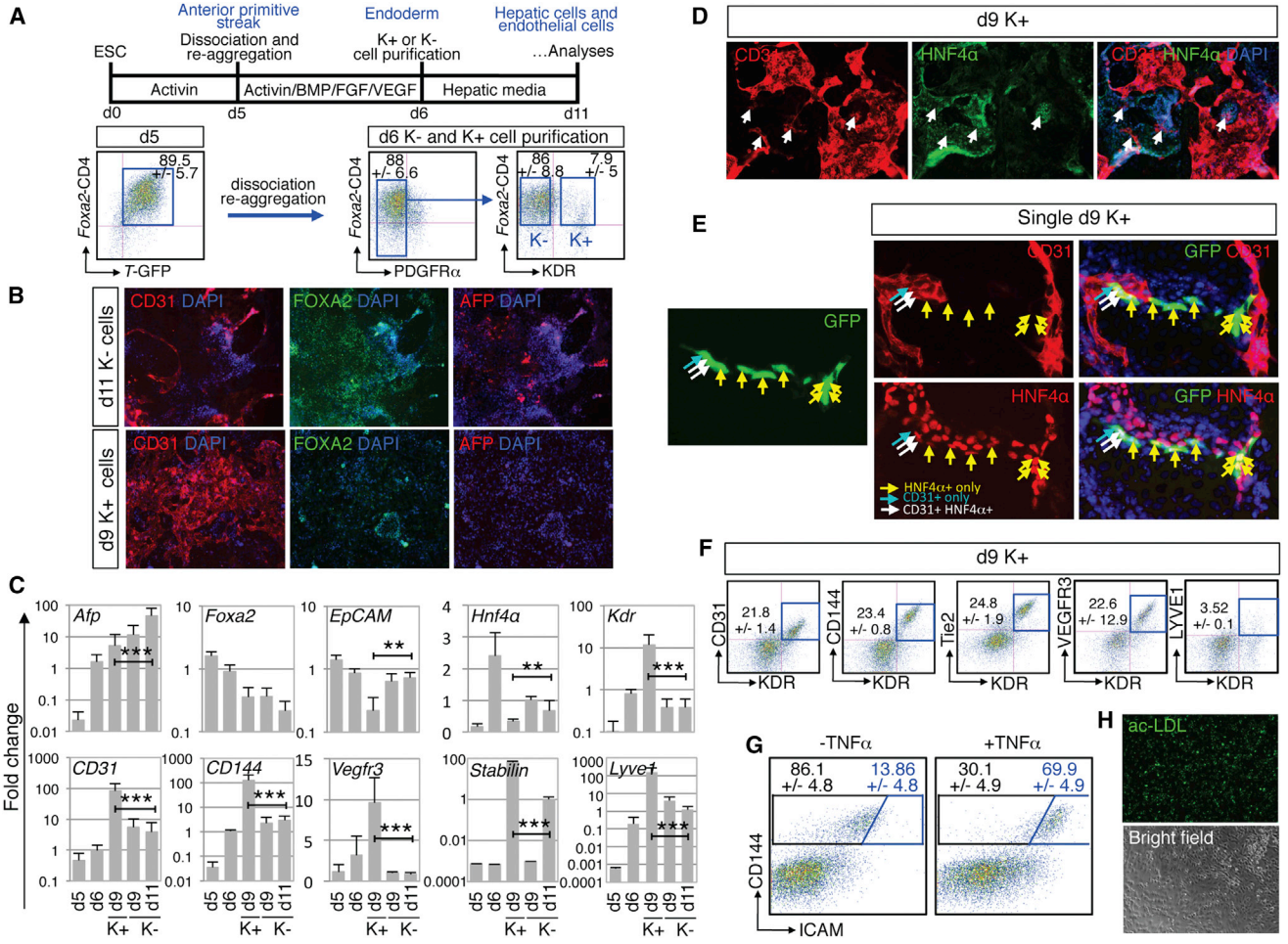


**Figure 3. Generation of ECs from Mouse ESC-Derived KDR+ FOXA2+ Endoderm Cells**

(A) Illustration of the mouse ESC hepatic differentiation protocol. Flow analysis from day 5 and day 6 EBs (n = 3) is shown.

(B) IF at day 11 from K− sorted cells and at day 9 from K+ sorted cells (×100).

(C) Relative transcript levels in day 5 EBs, day 6 EBs, K+ cells (at day 9), and K− cells (at day 9 and 11) (n = 3 independent experiments). Note that most y axes are in log scale.

(D) IF of K+ cells at day 9 of differentiation showing clusters of cells expressing both HNF4α and CD31 (×100, arrows).

(E) IF of HNF4α and CD31 of one GFP+ clone obtained from clonal assay of K+ cells (×200).

(F) Flow analysis of day 9 K+ cells (n = 3).

(G) Flow analysis for ICAM and CD144 expression of the K+ cells treated or not for 18 hr with TNF-α (n = 3).

(H) Images of ac-LDL incorporation by K+ cells (×200).

cells within the Activin A-induced EBs expressed *T*-GFP and high levels of *Foxa2*-CD4, indicative of anterior primitive streak-like cells (Figure 3A), as previously shown (Gouon-Evans et al., 2006). Following EB dissociation, cells were subjected to reaggregation in the presence of Activin A to maintain endoderm fate, bone morphogenetic protein 4 (BMP-4) and basic fibroblast growth factor (bFGF) to induce hepatic specification, and VEGF to promote EC survival (Gouon-Evans et al., 2006). One day later, most of the cells maintained expression of *Foxa2*-CD4. To exclude potential contamination with mesoderm and mesendoderm cells, the *T*-GFP+ cells and PDGFRα+ cells, respectively, were sorted out from the *Foxa2*-CD4+ cells that were subsequently analyzed for KDR expression. Among the *Foxa2*-CD4+PDGFRα− cells, a subset of cells expressed KDR (7.9% ± 5%). Both *Foxa2*-CD4+PDGFRα-KDR− cells (hereafter termed "K− cells") and *Foxa2*-CD4+PDGFRα-KDR+ cells (hereafter termed "K+ cells") were purified by FACS (Figure 3A) with purity greater that 95% for K− cells and higher than 85% for K+ cells. The latter were slightly contaminated with *Foxa2*-CD4+ but not with *Foxa2*-CD4-KDR+ cells (Figure S2B). Sorted cells were further cultured

to evaluate their hepatic and endothelial fate capacity by IF (Figures 3B and S2C) and quantitative PCR (qPCR) (Figure 3C).

K− cells maintained expression of FOXA2 following 5 days of culture and began to express α-fetoprotein (AFP), one of the first markers indicative of hepatic specification (Figure 3B). In contrast, FOXA2 was less expressed, and AFP protein was almost absent in differentiated K+ cell cultures (Figure 3B). CD31 was much more abundant in K+ cell cultures than in K− cultures. Thus, K+ cells have a propensity to specify into ECs and the K− cells into hepatic cells. These distinct fates of the K− and K+ populations were confirmed by qPCR analyses (Figure 3C). *Afp* transcript levels were detected in day 6 endoderm EBs following hepatic specification of the day 5 anterior primitive streak-like cells as expected. These levels were strongly upregulated over time in purified K− cells. The endoderm *Foxa2* transcript levels decreased with time as both purified populations differentiate. It is noteworthy that *Foxa2* transcript levels were similar at day 9 of differentiation in both K− and K+ populations, although FOXA2 protein was preferably expressed in K− hepatic cultures, reminiscent of the endoderm origin of CD31+ ECs derived from K+ cells. Similarly, levels of *Hnf4α* are detected in day 9 K+ cultures that are mainly composed of CD31+ ECs. Levels of *Hnf4α* decreased by only 50% as compared to those from day 11 K− cultures mainly composed of hepatic cells. Consistent with the hepatic identity of the K− cells, levels of the epithelial marker *EpCAM* remained similar in K− differentiated cells to those found in day 5 endoderm progenitors and day 6 endoderm population. However, these levels decreased dramatically in differentiated K+ cells and were inversely correlated with levels of the endothelial markers *Kdr*, *CD31*, and *CD144* (*VE-Cadherin*), supporting the endothelial potential of the K+ cells. Similar to the human endoderm-derived ECs, the mouse ECs derived from the K+ cells are highly enriched for the sinusoidal endothelial markers *Lyve-1*, *Vegfr3*, and *Stabilin*, suggesting the sinusoidal identity of these ECs.

IF for HNF4α and CD31 on day 9 differentiated K+ cells confirmed the qPCR data (Figures 3D and S2D). K+ cells derived both HNF4α+ hepatic endoderm cells and CD31+ ECs. Most interestingly, we found clusters of cells coexpressing HNF4α and CD31 (Figure 3D, arrows), implying the bipotential fate of K+ cells to differentiate into both hepatic endoderm and the endothelial lineage.

To provide definitive evidence for the endothelial fate of K+ endoderm cells, a clonal assay was used to show that single K+ endoderm cells give rise to both HNF4α+ hepatic endoderm cells and CD31+ ECs. In this assay, HNF4α was used as a marker because it is not expressed in ECs but strictly activated in the liver bud epithelium (Parviz et al., 2003). An antibody against HNF4α excluded any misinterpretation of the committed endoderm cells. Single GFP+K+ cells were isolated at day 6 of differentiation and cocultured with non-GFP-tagged endoderm cells to provide the GFP-tagged K+ cells an appropriate environment for cell survival and differentiation. Out of 768 wells plated with single cells, 233 contained a GFP+ clone following 3 days of culture (Figures S2E and S2F). Of the GFP+ colonies, 80.3% expressed the endothelial marker CD31, supporting the endothelial fate of K+ endoderm cells. Of the GFP+ colonies, 4.3% contained HNF4α+ hepatic endoderm cells, consistent with the endoderm origin of K+ cells. Most importantly, 2.6% of GFP+ clones were composed of both CD31+ ECs and HNF4α+ hepatic endoderm cells (Figures 3E, S2E, and S2F), validating the endoderm origin of the CD31+ ECs derived from K+ endoderm cells. Within these GFP+ clones, we identified a few cells that coexpressed HNF4α and CD31 (Figure 3E), supporting further the endoderm origin of the K+ cell-derived ECs.

Flow cytometry (flow) analyses confirmed the endothelial phenotype of the K+ differentiated cells and showed that following 3 days of culture, the K+ cells generated on average 25% of ECs that coexpressed KDR with CD31, CD144, TIE2, or VEGFR3 (Figure 3F). Membrane expression of LYVE1 by 3% of K+ cells was confirmed by flow (Figure 3F) and IF (Figure S2G).

To evaluate functionality of the K+ population-derived ECs, we performed the four in vitro functional assays described above for human ECs. The vast majority of CD144+ ECs induced ICAM expression following TNF-α stimulation (Figure 3G). They showed the ability to uptake ac-LDL (Figure 3H), migrate in a wound-healing assay (Figure S2H), and form tube-like structures in Matrigel (Figure S2I). Because differentiated K+ cell cultures were not solely composed of CD31+ ECs, the EC identity of the migrating cells was confirmed by IF for CD31 in the wound-healing (Figure S2H) and Matrigel (Figure S2I) assays. Similar to the human system, mouse ESC-derived endoderm gives rise to ECs from a KDR+FOXA2+-expressing progenitor cell.

## FOXA2+ Cells Contribute In Vivo to the Development of a Subset of ECs in Mouse Fetal Livers

We next probed the existence of FOXA2+ endoderm cell-derived ECs using a *Foxa2* lineage-tracing mouse model, obtained by crossing the heterozygous *Foxa2*-iCre mouse (Horn et al., 2012) with the homozygous reporter-enhanced yellow fluorescent protein (YFP) mouse, in which YFP is ubiquitously expressed under the *Rosa26* promoter, only after Cre recombinase excises the STOP cassette flanked by LoxP sites (Srinivas et al., 2001). The *Foxa2*-iCre mice faithfully mark cells that express FOXA2 from the anterior primitive streak of E7.5 embryos, in foregut, hindgut, and midgut endoderm, as well as in the heart,

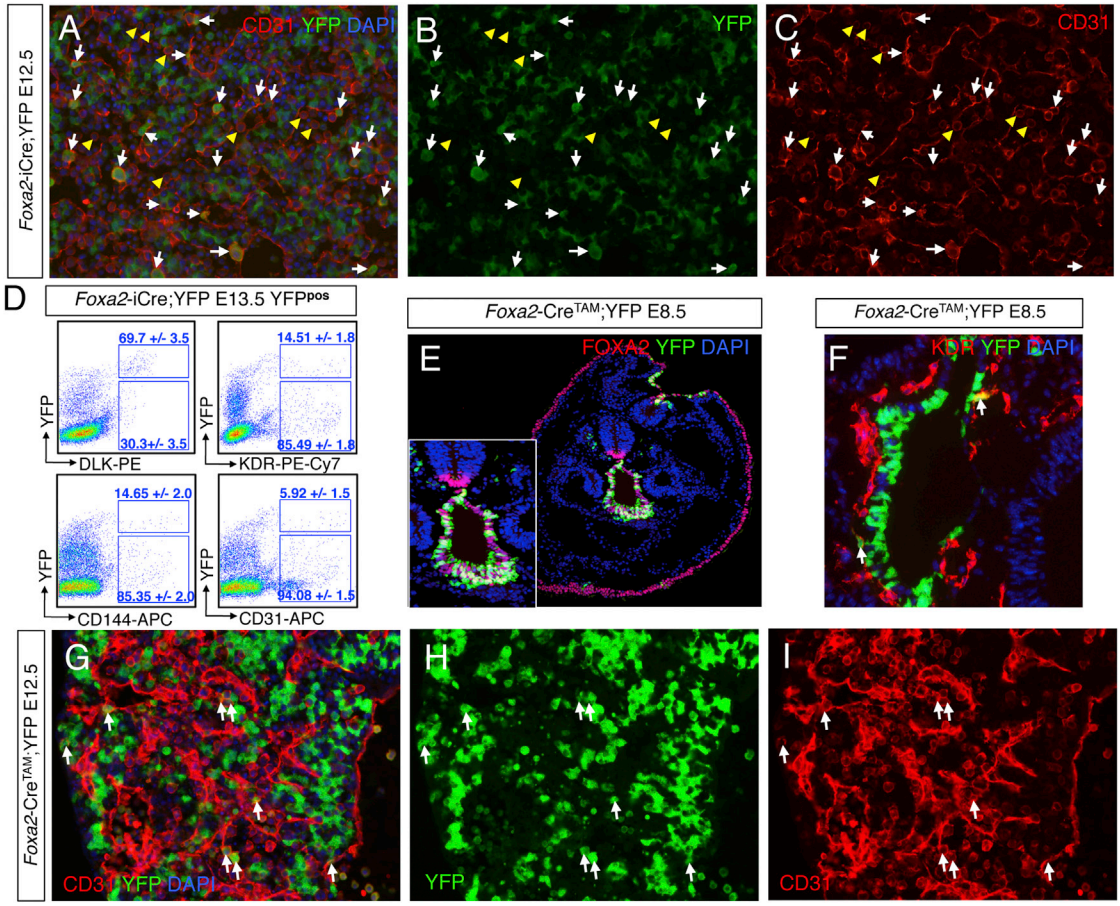


**Figure 4. FOXA2+ Cell Contribution to Fetal Liver ECs in Two *Foxa2* Lineage-Tracing Mouse Models**

(A–C) IF of fetal liver sections from E12.5 YFP$^{pos}$ embryos of *Foxa2*-iCre;YFP mice (×200). White arrows indicate the YFP+CD31+ ECs, and yellow arrowheads indicate the YFP-CD31+ hematopoietic cells.

(D) Flow analyses from four E13.5 YFP$^{pos}$ fetal livers and one E13.5 YFP$^{neg}$ fetal liver of *Foxa2*-iCre;YFP mice. Numbers indicate the mean ± SD of the percentage of cell populations in each gate for four YFP$^{pos}$ embryos.

(E) FOXA2 and YFP IF on E8.5 embryo section of *Foxa2*-Cre$^{TAM}$;YFP mice. Large image shows the tiling of a whole E8.5 embryo. The small image is a close-up of the foregut endoderm (×100).

(F) IF of YFP and KDR at E8.5 of *Foxa2*-Cre$^{TAM}$;YFP mice (×200). White arrows indicate rare YFP+KDR+ cells.

(G–I) IF for YFP and CD31 of E12.5 fetal liver sections from *Foxa2*-Cre$^{TAM}$;YFP mice (×200). White arrows indicate few YFP+CD31+ ECs.

notochord, and the floorplate of the developing neural tube in E9.5 embryos (Horn et al., 2012).

Despite the broad expression of FOXA2 in early embryogenesis, YFP marks specifically FOXA2+ hepatoblasts (Figure S3A, dotted area) that are positive for AFP (Figure S3B, consecutive section of A, dotted area) and unspecified foregut endoderm cells (Figure S3A, arrow) as the liver bud develops. The presence of FOXA2 protein in E9.5 liver buds was accurately recapitulated by YFP IF (Figure S3A) revealing the high FOXA2 tracking efficiency. To investigate the contribution of FOXA2+ cells to the endothelial lineage, co-IF for CD31 and YFP was performed on sections from E9.5 liver buds when hepatoblasts began to intermingle with ECs. Most of the CD31+ ECs were negative for YFP suggesting their mesodermal origin, although rare CD31+YFP+ cells were detected (Figures S3C–S3E arrows). In contrast, because the fetal liver expanded further at E12.5, many YFP+ CD31+ ECs were visualized (Figures 4A–4C, 20 arrows). Most of these YFP+ ECs were evenly integrated to the hepatic endothelial network, most likely the primitive sinusoids that are well established at that time. IF for AFP on consecutive slides indicated that all YFP+CD31+ cells were negative for AFP, confirming their committed endothelial phenotype (Figures S3B–S3E for E9.5, and Figures S3F–S3I for E12.5). The identity of the FOXA2+ cell-derived ECs was supported by the detection of YFP+KDR+ cells integrated into the E12.5 liver vasculature network (Figures S3J–S3L).

To quantify the contribution of FOXA2+ cells to the hepatic and EC populations, flow analyses were performed for coexpression of YFP with the hepatic cell surface marker Delta-like 1 homolog (DLK)/Pref-1 (Tanimizu et al., 2003) and endothelial markers CD31, KDR, and CD144 in dissociated E13.5 fetal livers (Figures 4D and S4A). The vast majority of DLK+ hepatoblasts was positive for YFP indicating efficient lineage tracing. About 15% of the CD144+KDR+ EC population within E13.5 fetal livers was YFP+, supporting the endoderm origin of this subset of ECs. The remaining ~85% of the total EC population was negative for YFP, consistent with a mesodermal origin of these ECs. CD31 expression confirmed the presence of YFP+ ECs, although with a lower percentage than those from the CD144 or KDR populations (5.92% ± 1.5%). This was expected because CD31 also marks some hematopoietic cells in mouse fetal livers that appeared on E12.5 fetal liver sections as round cells with weaker expression for CD31 (Figures 4A–4C, arrowheads) and as a $CD31^{low}$ population on flow plots (Figure 4D). The *Foxa2* lineage-tracing mouse study supports the existence of a subset of ECs derived from endoderm cells within the developing fetal liver.

Because Foxa2 is not solely restricted to endoderm in early embryogenesis, we further demonstrated the endoderm origin of a subset of hepatic fetal ECs using a more restrictive mouse model for fate mapping FOXA2+ endoderm cells: the tamoxifen-inducible *Foxa2*-$Cre^{TAM}$ line (Park et al., 2008). Injection of a single dose of tamoxifen at E6.75 resulted in tracking specifically FOXA2+ endoderm cells at E8.5 (Figures 4E and S4B) and hepatoblasts of the liver bud at E9.5 (Figures S4C and S4D) excluding tracing of any mesodermal derivatives. In this mouse model, a few KDR+YFP+ endoderm cells were found in E8.5 within the foregut endoderm (Figures 4F and S4B) and may represent progenitors for the endoderm-derived ECs observed at later stages. Rare YFP+ ECs coexpressing either CD31 or KDR were detected in E9.5 liver buds (Figures S4E and S4F, two arrows), whereas they were numerous in the E12.5 fetal liver (Figures 4G–4I and S4G–S4J, arrows).

## DISCUSSION

We provide evidence that endoderm-derived progenitors contribute to a subpopulation of hepatic ECs in the developing liver. The endoderm-derived ECs intermingle with the mesoderm-derived EC network developed by angiogenesis from the initial primitive vascular plexus. We identified the endoderm-derived endothelial progenitors by expression of the endoderm marker FOXA2 and the cell surface receptor KDR in both human and mouse ESC differentiation cultures. Lineage-tracing studies in the mouse embryo demonstrated that KDR is expressed not only on vascular and hematopoietic progenitors but also on a broad spectrum of other mesodermal progenitors that give rise to cardiac and skeletal muscle cells (Ema et al., 2006; Motoike et al., 2003). Other studies redefined the KDR-expressing cell as a bipotent progenitor for endothelial and hematopoietic cells in mouse embryos and hESC cultures, identified as the hemangioblast (Huber et al., 2004; Kennedy et al., 2007). Similarly, a bipotent KDR+ progenitor can give rise to both ECs and cardiomyocytes in the developing heart (Kattman et al., 2006; Yang et al., 2008). All these KDR+ progenitors are of mesodermal origin. Our previous study provided the first evidence for the existence of a KDR+ progenitor for liver, an endoderm derivative (Goldman et al., 2013). Given the well-documented studies on the bipotentiality of a KDR+ progenitor for the EC lineage and mesodermal derivatives, it should perhaps not be surprising that we were able to document the bipotentiality of an endoderm-derived KDR+ progenitor for hepatic endoderm cells and ECs using clonal assays. Similar to the hemangioblast or the bipotent endothelial-cardiomyocyte progenitor, we demonstrated the ability of single mouse KDR+FOXA2+ endoderm cells to give rise to both HNF4α+ hepatic endoderm and CD31+ ECs. Detection of CD31+ ECs coexpressing HNF4α from mouse and hESC hepatic differentiation cultures and the developing human fetal liver specimens further supports the existence of endoderm-derived ECs in fetal liver development. The inducible *Foxa2* lineage-tracing studies verified the endoderm origin of a subset of hepatic ECs. In the future, in vivo strategies may be capable of demonstrating the dynamic transition of endoderm cells turning off endoderm markers and developing into hepatic ECs while turning on blood vessel markers, in order to further confirm and define mechanisms by which endoderm generates ECs. Alternatively, single-cell RNA-sequencing studies might be used to capture a molecular profile of endoderm cells that are transitioning to an EC fate.

The functional specificity of ECs forming the microcirculation of organs has long been appreciated and recently defined molecularly by Nolan et al. (2013). The characterization of the KDR+ endoderm cell-derived ECs generated in mouse and hESC cultures suggests that those are the specialized sinusoidal ECs of the fetal liver. Likewise, two mesoderm-derived organs, the blood and heart, develop their own ECs from a common KDR+ progenitor for hematopoietic cells or cardiomyocytes, respectively. It is tempting to speculate that functional specificity of microvascular ECs is committed very early during organogenesis and ascribed to a common progenitor for the main cell component of the organ and the specialized ECs. Previous studies in blood and heart development and our work in liver development would suggest that this common progenitor expresses KDR. A deeper understanding of the

origin of the liver vascular heterogeneity should advance the fields of liver development and regeneration.

## EXPERIMENTAL PROCEDURES

### Human and Mouse ESC Hepatic Differentiation and Cell Sorting

hESCs (HES-2) were differentiated into the hepatic lineage as previously described (Goldman et al., 2013). At day 5 of differentiation, CXCR4+cKIT+KDR-PDGFRα− endoderm cells were isolated with a FACSAria Cell Sorter (BD Biosciences) and cultured in hepatic media as previously defined (Han et al., 2011).

The mouse ESC line *T*-GFP/*Foxa2*-CD4 was described (Gouon-Evans et al., 2006). ESCs were cultured at 30,000 cells/ml for EB formation in serum-free differentiation (SFD) media (Gouon-Evans et al., 2006). Day 2 EBs were dissociated, and cells (40,000 cells/ml) were reaggregated in SFD media with Activin A (100 ng/ml; PeproTech). Day 5 EBs were dissociated and reaggregated with SFD media with Activin A (100 ng/ml), BMP-4 (10 ng/ml), VEGF (10 ng/ml), and bFGF (10 ng/ml; Invitrogen). Day 6 aggregates were dissociated with 0.25% trypsin/EDTA. Purified populations were further cultured in hepatic media. All cytokines except Activin A and bFGF were purchased from R&D Systems.

### Mice

The *Foxa2* lineage-tracing mouse model was obtained by crossing the heterozygous *Foxa2*-iCre mice (Horn et al., 2012) and the homozygous reporter *Rosa26*-$^{loxP}$STOP$^{loxP}$-eYFP mice (Srinivas et al., 2001). The inducible *Foxa2*-Cre$^{TAM}$ mouse model was obtained from Jackson Laboratory (stock number 008464) and crossed with the YFP reporter mice. The use of mouse models in these experiments received Institutional Animal Care and Use Committee approval.

## SUPPLEMENTAL INFORMATION

Supplemental Information includes Supplemental Experimental Procedures, four figures, and four tables and can be found with this article online at http://dx.doi.org/10.1016/j.stemcr.2014.08.009.

## AUTHOR CONTRIBUTIONS

O.G. designed and performed experiments related to human studies, contributed to some mouse studies, and wrote the manuscript. S.H. designed and performed the mouse studies and wrote the manuscript. W.H. performed cell transplantations and edited the manuscript. V.J.d.V. provided human fetal liver specimens. G.U. provided human fetal liver specimens and edited the manuscript. H.L. provided the Foxa2-iCre mouse, helped in designing mouse experiments, and edited the manuscript. V.G.-E. designed all experiments and wrote the manuscript.

## ACKNOWLEDGMENTS

We thank Dr. Darrell Kotton for providing the *Ef1α*− GFP lentivirus-tagged mouse ESC line, Catherine Delmau for helpful advice for the artery femoral injury assay, and the Mouse Genetics and Gene Targeting SRF from Icahn School of Medicine at Mount Sinai for the rederivation of the *Foxa2*-iCre mice. The authors would like to thank Dr. Todd Evans for critical reading of the manuscript. This work was supported by the Black Family Stem Cell Institute and the National Institute of Diabetes and Digestive and Kidney Diseases for the mouse study (R01DK087867-01 to V.G.-E.).

Received: July 24, 2014
Revised: August 13, 2014
Accepted: August 14, 2014
Published: September 18, 2014

## REFERENCES

Ding, B.S., Nolan, D.J., Butler, J.M., James, D., Babazadeh, A.O., Rosenwaks, Z., Mittal, V., Kobayashi, H., Shido, K., Lyden, D., et al. (2010). Inductive angiocrine signals from sinusoidal endothelium are required for liver regeneration. Nature *468*, 310–315.

Ema, M., Takahashi, S., and Rossant, J. (2006). Deletion of the selection cassette, but not cis-acting elements, in targeted Flk1-lacZ allele reveals Flk1 expression in multipotent mesodermal progenitors. Blood *107*, 111–117.

Goldman, O., Feraud, O., Boyer-Di Ponio, J., Driancourt, C., Clay, D., Le Bousse-Kerdiles, M.C., Bennaceur-Griscelli, A., and Uzan, G. (2009). A boost of BMP4 accelerates the commitment of human embryonic stem cells to the endothelial lineage. Stem Cells *27*, 1750–1759.

Goldman, O., Han, S., Sourrisseau, M., Dziedzic, N., Hamou, W., Corneo, B., D'Souza, S., Sato, T., Kotton, D.N., Bissig, K.D., et al. (2013). KDR identifies a conserved human and murine hepatic progenitor and instructs early liver development. Cell Stem Cell *12*, 748–760.

Gouon-Evans, V., Boussemart, L., Gadue, P., Nierhoff, D., Koehler, C.I., Kubo, A., Shafritz, D.A., and Keller, G. (2006). BMP-4 is required for hepatic specification of mouse embryonic stem cell-derived definitive endoderm. Nat. Biotechnol. *24*, 1402–1411.

Han, S., Dziedzic, N., Gadue, P., Keller, G., and Gouon-Evans, V. (2011). An endothelial cell niche induces hepatic specification through dual repression of Wnt and Notch signaling. Stem Cells *29*, 217–228.

Horn, S., Kobberup, S., Jørgensen, M.C., Kalisz, M., Klein, T., Kageyama, R., Gegg, M., Lickert, H., Lindner, J., Magnuson, M.A., et al. (2012). Mind bomb 1 is required for pancreatic β-cell formation. Proc. Natl. Acad. Sci. USA *109*, 7356–7361.

Huber, T.L., Kouskoff, V., Fehling, H.J., Palis, J., and Keller, G. (2004). Haemangioblast commitment is initiated in the primitive streak of the mouse embryo. Nature *432*, 625–630.

Kattman, S.J., Huber, T.L., and Keller, G.M. (2006). Multipotent flk-1+ cardiovascular progenitor cells give rise to the cardiomyocyte, endothelial, and vascular smooth muscle lineages. Dev. Cell *11*, 723–732.

Kennedy, M., D'Souza, S.L., Lynch-Kattman, M., Schwantz, S., and Keller, G. (2007). Development of the hemangioblast defines the onset of hematopoiesis in human ES cell differentiation cultures. Blood *109*, 2679–2687.

Motoike, T., Markham, D.W., Rossant, J., and Sato, T.N. (2003). Evidence for novel fate of Flk1+ progenitor: contribution to muscle lineage. Genesis *35*, 153–159.

Nolan, D.J., Ginsberg, M., Israely, E., Palikuqi, B., Poulos, M.G., James, D., Ding, B.S., Schachterle, W., Liu, Y., Rosenwaks, Z., et al. (2013). Molecular signatures of tissue-specific microvascular endothelial cell heterogeneity in organ maintenance and regeneration. Dev. Cell *26*, 204–219.

Nonaka, H., Tanaka, M., Suzuki, K., and Miyajima, A. (2007). Development of murine hepatic sinusoidal endothelial cells characterized by the expression of hyaluronan receptors. Dev. Dyn. *236*, 2258–2267.

Park, E.J., Sun, X., Nichol, P., Saijoh, Y., Martin, J.F., and Moon, A.M. (2008). System for tamoxifen-inducible expression of cre-recombinase from the Foxa2 locus in mice. Dev. Dyn. *237*, 447–453.

Parviz, F., Matullo, C., Garrison, W.D., Savatski, L., Adamson, J.W., Ning, G., Kaestner, K.H., Rossi, J.M., Zaret, K.S., and Duncan, S.A. (2003). Hepatocyte nuclear factor 4alpha controls the development of a hepatic epithelium and liver morphogenesis. Nat. Genet. *34*, 292–296.

Patan, S. (2004). Vasculogenesis and angiogenesis. Cancer Treat. Res. *117*, 3–32.

Roskams, T., and Desmet, V. (2008). Embryology of extra- and intrahepatic bile ducts, the ductal plate. Anat. Rec. (Hoboken) *291*, 628–635.

Shiojiri, N., Niwa, T., Sugiyama, Y., and Koike, T. (2006). Preferential expression of connexin37 and connexin40 in the endothelium of the portal veins during mouse liver development. Cell Tissue Res. *324*, 547–552.

Srinivas, S., Watanabe, T., Lin, C.S., William, C.M., Tanabe, Y., Jessell, T.M., and Costantini, F. (2001). Cre reporter strains produced by targeted insertion of EYFP and ECFP into the ROSA26 locus. BMC Dev. Biol. *1*, 4.

Sugiyama, Y., Takabe, Y., Nakakura, T., Tanaka, S., Koike, T., and Shiojiri, N. (2010). Sinusoid development and morphogenesis may be stimulated by VEGF-Flk-1 signaling during fetal mouse liver development. Dev. Dyn. *239*, 386–397.

Tanimizu, N., Nishikawa, M., Saito, H., Tsujimura, T., and Miyajima, A. (2003). Isolation of hepatoblasts based on the expression of Dlk/Pref-1. J. Cell Sci. *116*, 1775–1786.

Yang, L., Soonpaa, M.H., Adler, E.D., Roepke, T.K., Kattman, S.J., Kennedy, M., Henckaerts, E., Bonham, K., Abbott, G.W., Linden, R.M., et al. (2008). Human cardiovascular progenitor cells develop from a KDR+ embryonic-stem-cell-derived population. Nature *453*, 524–528.

**Stem Cell Reports, Volume *3***

**Supplemental Information**

# Endoderm Generates Endothelial Cells during Liver Development

**Orit Goldman, Songyan Han, Wissam Hamou, Vanina Jodon de Villeroche, Georges Uzan, Heiko Lickert, and Valerie Gouon-Evans**

**SUPPLEMENTAL FIGURES AND LEGENDS**

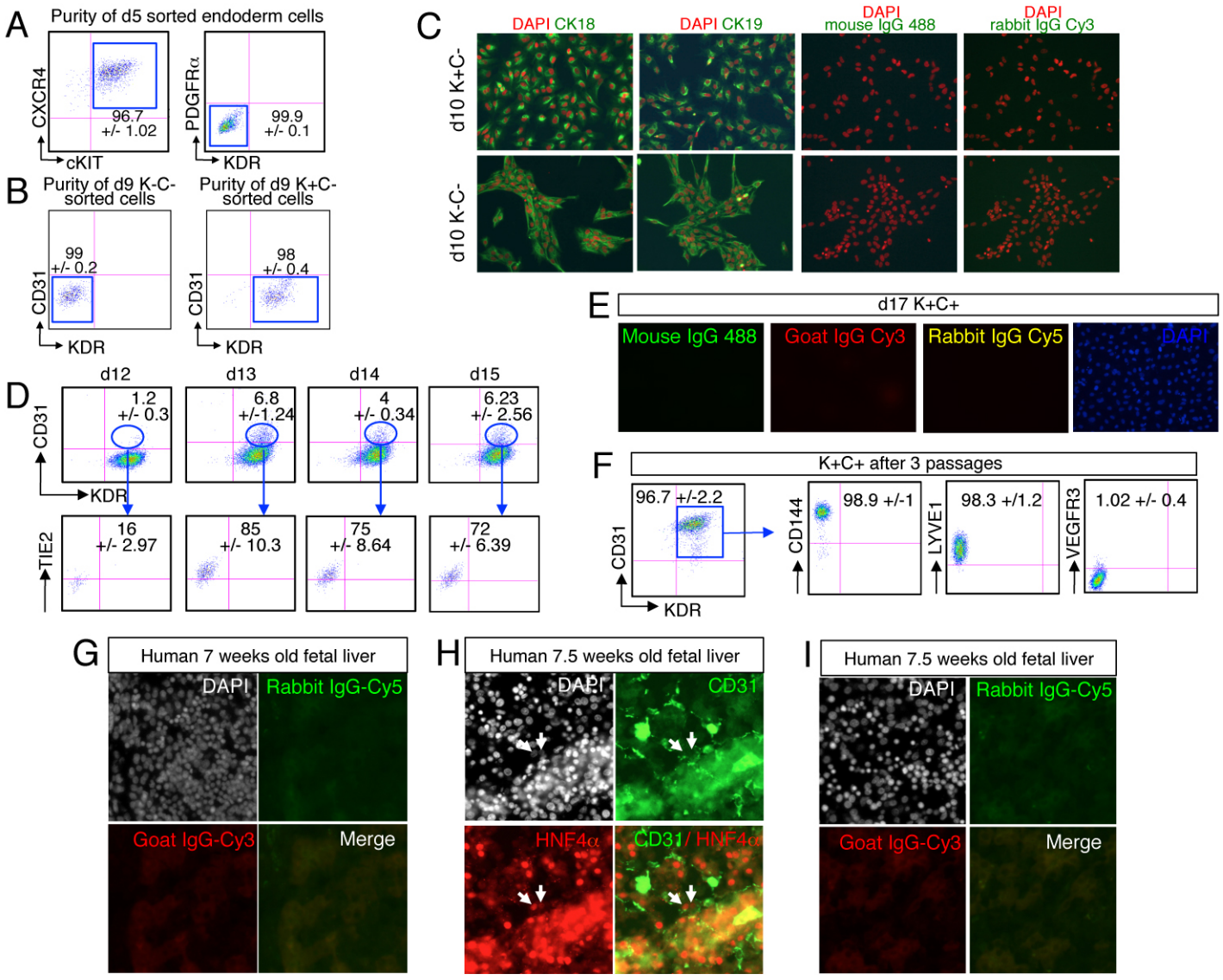


**Figure S1 for Figure 1: Characterization of ECs from human ESC-derived KDR+ endoderm cells and human fetal livers.**

(A) Representative flow cytometry analyses of the purity of day 5 endoderm populations isolated within the CXCR4+cKIT+KDR-PDGFRα- fraction, and (B) of the K+C- and K-C- populations isolated from day 9 hepatic cultures. Numbers represent means +/- SD of n=10 independent experiments. (C) Immunostaining using antibodies against CK18 and CK19, and IgG controls of K+C- and K-C- populations purified at day 9 and cultured for 1 day (day10 of differentiation) in hepatic conditions (x200). (D) Flow cytometry analysis of day 12 to day 15 cultures obtained from day 9 isolated K+C- cells (n=3). (E) IgG controls for Figure 1H (x200). (F) Flow cytometry analysis from purified K+C+ cells after 3 passages (n=3). (G) IgG controls for Figure 1J. (x200). (H) Co-immunostainings for CD31 and HNF4α (x200), (I) and IgG controls (x200) on 7.5 weeks old human fetal liver sections.

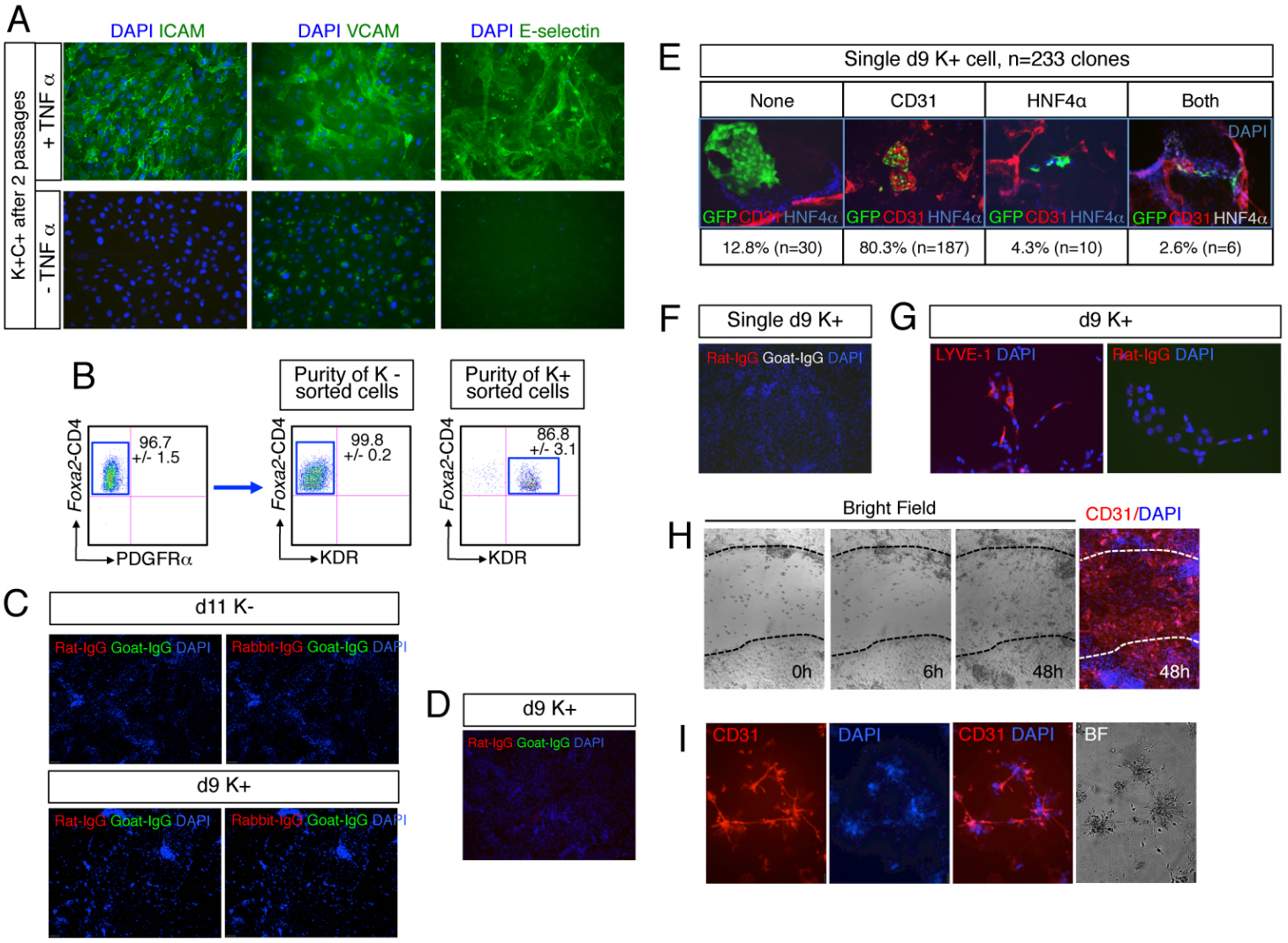


**Figure S2 for Figure 2 and 3: Characterization of ECs from human and mouse ESC-derived KDR+ endoderm cells.**

(A) Immunostaining of K+C+ cells after 2 passages using antibodies against ICAM, VCAM and E-selectin following TNFα activation (x200). (B) Representative flow cytometry analyses for the purity of day 6 K+ and K- populations isolated within the *Foxa2*-CD4+*T*-GFP-PDGFRα-KDR+ (named K+ cells) or *FoxA2*-CD4+*T*-GFP-PDGFRα-KDR- (named K- cells) fractions respectively. Numbers represent means +/- SD of n=3 independent experiments. (C) IgG controls counterstained with DAPI of immunostaining shown in Figure 3B (x200). (D) IgG control for immunostaining of Figure 3D (X200). (E) Summary of the cell fate of 233 clones generated in clonal assay of K+ cells at day 9 of differentiation (X200). (F) IgG control for immunostaining of the clonal assay (X100). (G) LYVE1 immunostaining and IgG control on day 9 K+ cells (X200). (H) Wound healing assay of K+ cells. Migrating endothelial cells were identified following immunostaining for CD31 in the dish (x200). (I) Tube formation assay in matrigel by K+ cells. Immunostaining for CD31 of K+ cells was also performed (x200).

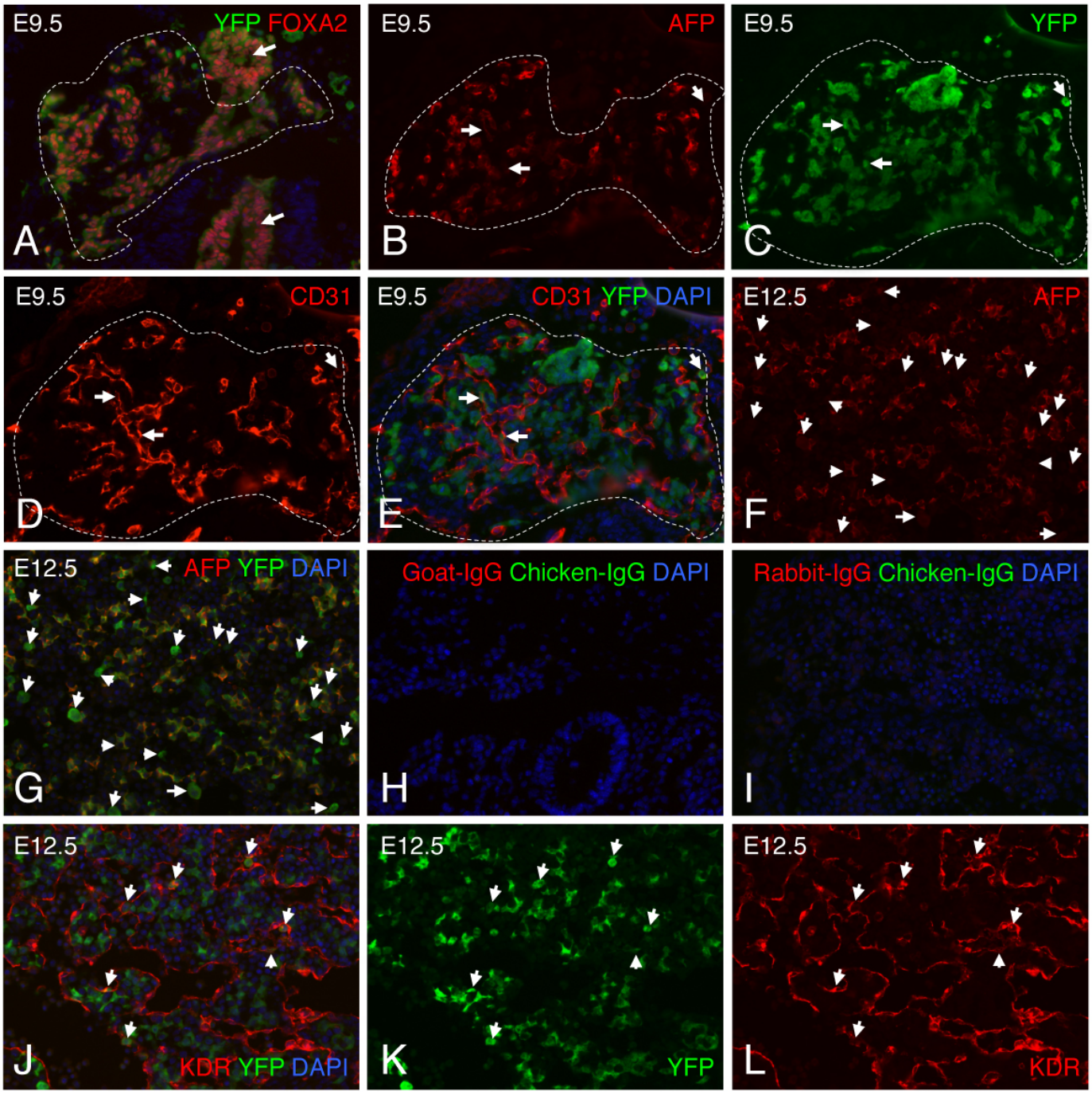


**Figure S3 for Figure 4: *Foxa2*-iCre lineage tracing mouse analyses.**

(A-E) Immunostaining of E9.5 embryo sections of *Foxa2*-iCre;YFP mice for YFP, FOXA2, AFP and CD31 (A: x100, B-E: X200). (B) represents the liver bud on the consecutive section from (A). (C-E) represent the same field of the liver bud on the same section with single (C, D) or merged staining (E) on the following consecutive section from (B). (F-G) Immunostaining of the same E12.5 embryo fetal liver section shown in Figure 4A-C for YFP and AFP indicating that all CD31+YFP+ cells (arrows) are negative for AFP (x200). (H-I) Immunostainings with IgGs controls for KDR, CD31 and YFP antibodies on E12.5 fetal liver sections. (J-L) Immunostaining for YFP, KDR and DAPI of a consecutive section from the E12.5 embryo shown in Figure 4A-C (X200). Arrows indicate KDR+YFP+ cells.

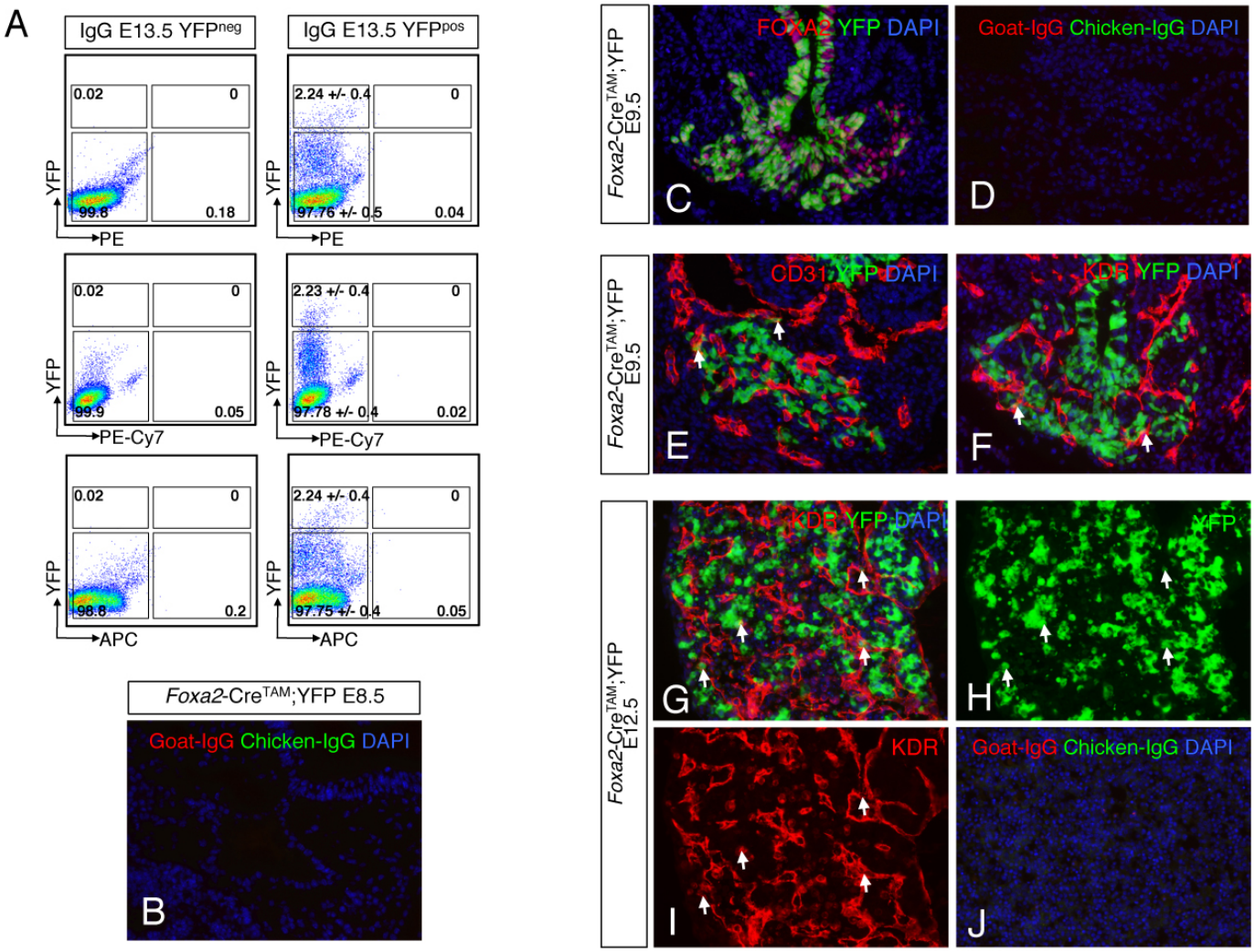


**Figure S4 for Figure 4: *Foxa2*-iCre and *Foxa2*-Cre$^{TAM}$ lineage tracing mouse model analyses.**

(A) IgG controls for flow cytometry analyses of E13.5 fetal liver cells from *Foxa2*-iCre;YFP mice. Numbers indicate the means +/- SD of the percentage of cells in the respective gates for n=4 embryos YFP$^{neg}$ and 1 embryo YFP$^{pos}$. (B) IgG controls for immunostaining of E8.5 *Foxa2*-Cre$^{TAM}$;YFP embryos for Figure 4E. (C-D) FOXA2 and YFP immunostaining and IgG controls of E9.5 liver bud section of *Foxa2*-Cre$^{TAM}$;YFP mice validating the high specificity of YFP mapping for FOXA2+ endoderm cells and hepatoblasts (x200). (E-F) Co-immunostaining for YFP and CD31 (E) or KDR (F) on liver bud section at E9.5 of *Foxa2*-Cre$^{TAM}$;YFP mice showing rare single endothelial cells originated from FOXA2+ endoderm progenitors (X200). (G-J) YFP and KDR immunostaining and IgG controls on E12.5 liver section of *Foxa2*-Cre$^{TAM}$;YFP mice showing cells co-expressing YFP and KDR (arrows, X200).

**SUPPLEMENTAL TABLES**

| Antibody | Species | Company | Cat. Number | Application | Dilution |
|---|---|---|---|---|---|
| CXCR4-PE | Mouse | R&D System | FAB170P | FC | 1/20 |
| cKit-PECy7 | Mouse | BD Biosciences | 339206 | FC | 1/20 |
| PDGF-FITC | Mouse | Caltag | K0148-4 | FC | 1/20 |
| KDR-647 | Mouse | BD Biosciences | 560495 | FC | 1/20 |
| CD31-FITC | Mouse | BD Biosciences | 555445 | FC | 1/100 |
| CD144-PE | Mouse | Beckman Coulter | A07481 | FC | 1/20 |
| TIE2-PE | Mouse | millipore | FCMAB404PE | FC | 1/100 |
| ICAM | Mouse | R&D System | BBA3 | FC | 1/20 |
| VCAM | Mouse | R&D System | BBA5 | FC | 1/20 |
| CK18 | Mouse | Sigma | C8541 | ICC | 1/100 |
| CK19 | Mouse | Dako | M0888 | ICC | 1/100 |
| HNF4$\alpha$ | Goat | SantaCruz | Sc-6556 | ICC | 1/100 |
| Mouse IgG | | Jackson Immunoresearch laboratories | 015-000-003 | FC | |
| CD31 | mouse | BD Biosciences | 555675 | ICC | 1/100 |
| KDR | Goat | R&D System | AF357 | ICC | 1/20 |
| CD31 | Rabbit | invitrogen | 550389 | IHC | 1/100 |
| vWF | rabbit | Dako | A0082 | ICC | 1/700 |
| Goat IgG | | Jackson Immunoresearch laboratories | 005-000-003 | ICC IHC | |
| Rabbit IgG | | Jackson Immunoresearch laboratories | 011-000-003 | ICC IHC | |
| Donkey anti mouse 488 | | Jackson Immunoresearch laboratories | A21202 | ICC IHC | 1/250 |
| Donkey anti goat Cy3 | | Jackson Immunoresearch laboratories | 705-165-147 | ICC IHC | 1/250 |
| Donkey anti mouse Cy3 | | Jackson Immunoresearch laboratories | 715-165-150 | ICC IHC | 1/250 |
| Donkey anti rabbit Cy5 | | Jackson Immunoresearch laboratories | 711-606-152 | ICC IHC | 1/250 |

**Table S1: Supplemental experimental procedures, antibodies against human proteins used in Figures 1, 2 and S1.**

| Antibody | Species | Company | Cat. Number | Application | Dilution |
|---|---|---|---|---|---|
| hCD4-APC | Mouse | Invitrogen | MHCD0405 | FC | 1/100 |
| PDGFRα-PE | Rat | eBioscience | 12-1401-81 | FC | 1/100 |
| KDR-PECy7 | Rat | BD Biosciences | 561259 | FC | 1/150 |
| CD31-APC | Rat | BD Biosciences | 551262 | FC | 1/100 |
| TIE2-PE | Rat | eBioscience | 12-5987-81 | FC | 1/100 |
| CD144-APC | Rat | eBioscience | 17-1441-80 | FC | 1/100 |
| DLK-PE | Rat | MBL | D187-5 | FC | 1/100 |
| ICAM-APC | Rat | R&D Systems | FAB796A | FC | 1/100 |
| FOXA2 | Goat | Santa cruz | Sc-6554 | ICC IHC | 1/50 |
| HNF4α | Goat | Santa cruz | Sc-6556 | ICC | 1/100 |
| AFP | Rabbit | Neomarkers | RB-365-A | ICC IHC | 1/200 |
| KDR | Goat | R&D Systems | AF644 | IHC | 1/30 |
| CD31 | Goat | R&D Systems | AF3628 | IHC | 1/30 |
| CD31 | Rat | BD | 557355 | ICC | 1/150 |
| LYVE1 | Rat | Santa cruz | Sc-65647 | ICC | 1/50 |
| GFP (YFP) | Chicken | Invitrogen | A10262 | IHC | 1/300 |
| Rat IgG | | Jackson Immunoresearch laboratories | 012-000-003 | ICC | |
| Goat IgG | | Jackson Immunoresearch laboratories | 005-000-003 | ICC IHC | |
| Rabbit IgG | | Jackson Immunoresearch laboratories | 011-000-003 | ICC IHC | |
| Chicken IgG-Y | | Jackson Immunoresearch laboratories | 003-000-003 | IHC | |
| Donkey anti chicken Cy3 | | Jackson Immunoresearch laboratories | 703-162-155 | IHC | 1/400 |
| Donkey anti goat A647 | | Jackson Immunoresearch laboratories | 705-605-147 | IHC | 1/400 |
| Donkey anti goat A488 | | Invitrogen | A11055 | ICC | 1/400 |
| Donkey anti rabbit A647 | | Jackson Immunoresearch laboratories | 711-606-152 | ICC IHC | 1/400 |
| Donkey anti rat cy3 | | Jackson Immunoresearch laboratories | 712-166-153 | ICC | 1/400 |

**Table S2: Supplemental experimental procedures, antibodies against mouse proteins used in Figures 3, 4, S2, S3 and S4.**

| Name | Forward | Reverse |
|---|---|---|
| *β-ACTIN* | 5'- TTTTTGGCTTGACTCAGGATTT-3' | 5'- GCAAGGGACTTCCTGTAACAAC-3' |
| *LYVE-1* | 5'- TGGGGATCACCCTTGTGAG-3' | 5'- AGCCATAGCTGCAAGTTTCAAA-3' |
| *VEGFR3* | 5'-TGCACGAGGTACATGCCAAC-3' | 5'-GCTGCTCAAAGTCTCTCACGAA-3' |
| *HNF4α* | 5'-CACGGGCAAACACTACGGT-3' | 5'-TTGACCTTCGAGTGCTGATCC-3' |

**Table S3: Supplemental experimental procedures, list of human primers for qPCR used in Figure 1.**

| Name | Forward | Reverse |
|---|---|---|
| *β-Actin* | 5'-TGAGCGCAAGTACTCTGTGTGGAT-3' | 5'-ACTCATCGTACTCCTGCTTGCTGA-3' |
| *Foxa2* | 5'-CTCTCTCTCCTTCAACGACTGCTTTCTC-3' | 5'-TTCCTTCAGTGCCAGTTGCTTCTC-3' |
| *EpCAM* | 5'-CGTGAGGACCTACTGGATCAT-3' | 5'-GTCCACGTCGTCTTGTGTTTT-3' |
| *HNF4α* | 5'- AAGGTGCCAACCTCAATTCATC -3' | 5'- CACATTGTCGGCTAAACCTGC -3' |
| *Afp* | 5'-GGAATGAAGCAAGCklkCCTGTGAACT -3' | 5'-AACTGGTGATGCATAGCCTCCTGT-3' |
| *Kdr* | 5'-TTTGGCAAATACAACCCTTCAGA-3' | 5'-GCTCCAGTATCATTTCCAACCA-3' |
| *CD31* | 5'-TGAAGACAGACCTCAAGCCAGCAA-3' | 5'-ACAGCTCAGACCTTAGGAAACCGT-3' |
| *CD144* | 5'-GTCGATGCTAACACAGGGAATG-3' | 5'-AATACCTGGTGCGAAAACACA-3' |
| *Lyve1* | 5'-CAGCACACTAGCCTGGTGTTA-3' | 5'-CGCCCATGATTCTGCATGTAGA-3' |
| *Vegfr3* | 5'-GGCAAATGGTTACTCCATGACC-3' | 5'-ACAACCCGTGTGTCTTCACTG-3' |
| *Stabilin* | 5'-AGCTGCTGCCTTTAATCCTCA-3' | 5'-ACTCCGTCTTGATGGTTAGAGTA-3' |

**Table S4: Supplemental experimental procedures, list of mouse primers for qPCR used in Figure 3.**

## SUPPLEMENTAL EXPERIMENTAL PROCEDURES

### Flow cytometry analyses

Cultured cells were dissociated with trypsin/EDTA or E13.5 fetal liver embryos were dissociated as previously described (Goldman et al., 2013). Cells were then immunostained with specific antibody (see Tables S1, S2) in PBS with BSA 0.1% at room temperature for 20 minutes. Cells were then analyzed using a LSRII flow cytometer (Becton Dickinson). Fluorochrome-labeled IgGs were used as controls for human CD31, VCAM, ICAM, E-selectin, Tie2, CD144, LYVE1 and VEGFR3 stainings. Absence of antibody was otherwise considered as control stainings as positive stainings were far away from the negative gate.

### Wound healing assay

Cells were expended in hepatic media. A starch was made with a cell culture tip and pictures were taken at different time points following further culture.

### Uptake of acetylated LDL

Cells were incubated for 6 hours with 15 ng/ml of LDL-ac-GFP (life sciences). Stained cells were visualized using a fluorescent microscope Leica.

### Vascular tube formation

250,000 human cells were seeded in a 12-well plate or 20,000 mouse cells were seeded in a 48-well plate coated with matrigel in EGM2 media (Lonza) with 50 ng/ml of VEGF (R&D). Pictures were taken 24 hours after seeding with a microscope Leica.

### Tumor necrosis factor assay

Cells were incubated during 18 hours with 10 ng/ml of TNFα (R&D system). Cells were then dissociated with trypsine/EDTA and immunostained with antibodies against ICAM or VCAM for 20minutes.

### Clonal assay

*Ef1α*- GFP lentivirus tagged mouse ESC line was differentiated into definitive endoderm similarly to the *T*-GFP/*Foxa2*-CD4 ESCs (Gift from Dr. Darrell Kotton, Boston University). At day 6 of differentiation, single alive GFP+FOXA2+KDR+PDGFRα- cells were isolated and cultured with 8,000 non-GFP-tagged day 6 differentiated ESCs (*T*-GFP/*Foxa2*-CD4) in 96 well plates in hepatic medium as previously described (Han et al., 2011). Hepatic endoderm and endothelial fate of the GFP+ clones was determined by HNF4α and CD31 immunostaining, respectively, 3 days after plating.

### In vivo ischemia assay

Adult NOD/SCID mice were injected with 50μl of 0.25 x$10^6$ human K+C- cells into 4 different points of a muscle in the area where the femoral artery was ligated as previously described (Vanneaux et al., 2010). Seven days after transplantation, 100μl GFP-labeled dextran (25mg/4ml; Life Technologies, NY) was injected through the carotid artery prior to sacrifice.

### Immunostainings

Adherent cells were fixed with 4% paraformaldehyde for 15 min and incubated for 30 minutes with Dako blocking buffer. Cells were permeabilized with Triton X-100 0.3%, incubated for 30 minutes with the Dako blocking buffer and stained with primary antibodies overnight at 4°C. The next morning, cells were then washed and incubated with secondary antibodies for 1 hour at room temperature and counterstained with DAPI. For co-staining with CD31, cells were first immunostained with CD31 overnight and then permeabilized prior to the second immunostaining (see Table S1 and S2 for the list of antibodies).

### Immunohistochemistry

E9.5 and E12.5 embryos were fixed for 2 hours with 4% PFA at 4°C, while muscle tissues or human fetal livers were fixed over night. Tissues were then washed with PBS for 3 times and dehydrated with 30% sucrose and embedded in OCT. Cryosections of 8-µm were blocked with 3% of donkey serum with or without permeabilization (for CD31 staining) in the presence of 0.3% Triton X-100, immunostained with primary antibodies (see Table S1 and S2) overnight at 4°C. Sections were then incubated for 1 hour with secondary antibodies (see Table S1 and S2) at room temperature and counterstained with DAPI. Sections were visualized using a fluorescent confocal microscope (Leica).

**RNA extraction and qPCR**

Total RNA was prepared with the RNeasy micro kit (Qiagen). RNA was reverse transcribed into cDNA using the Super Script-III First-strand Synthesis System kit (Invitrogen). qPCR was performed with the Roche system LC480. All experiments were done in triplicate using the Roche SYBR Green master mix. Relative quantification was calculated using the comparative threshold cycle (CT) method and was normalized against the ΔCT of the housekeeping gene β-actin. Melting curves for each gene were used to confirm homogeneity of the DNA product (see the list of primers in Table S3 and S4).

**Statistic analyses**

All numbers reflect means +/- SD for n independent experiments. Calculations were performed with the paired t-tests. Significance were defined as * $p< 0.05$ , ** $p<0.01$, and *** $p<0.001$***.

**SUPPLEMENTAL REFERENCES**

Vanneaux, V., El-Ayoubi, F., Delmau, C., Driancourt, C., Lecourt, S., Grelier, A., Cras, A., Cuccuini, W., Soulier, J., Lataillade, J.J., et al. (2010). In vitro and in vivo analysis of endothelial progenitor cells from cryopreserved umbilical cord blood: are we ready for clinical application? Cell Transplant 19, 1143-1155.